

# A Lifting Algorithm for Output-only Continuous Scan Laser Doppler Vibrometry

Shifei Yang<sup>1</sup>, Matthew S. Allen<sup>2</sup>

*University of Wisconsin-Madison, Madison, Wisconsin, 53706, USA*

Continuous Scan Laser Doppler Vibrometry (CSLDV) can greatly accelerate modal testing by continuously sweeping the measuring laser over the structure, effectively capturing the response of the structure at tens or even hundreds of points simultaneously. The authors recently extended this technique to the case where the input forces are unmeasured and random using harmonic power spectrum. This paper presents a variant on the proposed method that combines lifting, a resampling approach, with the output only algorithm. Lifting causes all of the peaks in the harmonic power spectrum to collapse onto a single peak for each mode, greatly simplifying modal parameter estimation. The proposed approach works by estimating and then lifting the harmonic correlation function, which is analogous to the impulse response of the system. The proposed algorithm is evaluated on a simulated beam and compared with the previous output only methods, indicating that the new approach gives comparable results to those of the previous methods but the data reduction is far simpler. The algorithm is then used to identify the first several modes of a parked wind turbine under wind excitation, capturing the deformation shape along one blade in detail. A new long range Remote Sensing Vibrometer (RSV) from PolyTec<sup>®</sup> was employed for these measurements. This new vibrometer allows the first several modes of the turbine to be captured, from a standoff distance of 77 meters without the retro-reflective tape applied to the turbine. The speckle noise in the measurements is found to be remarkably small, allowing a 36 Hz scan frequency to be employed, which corresponds to a surface velocity of the laser spot of more than 500 m/s.

## Nomenclature

CSLDV	=	Continuous-Scan Laser Doppler Vibrometry
EMP	=	Exponentially Modulated Periodic
HTF	=	Harmonic Transfer Function
HCF	=	linear Harmonic Correlation Function
pHCF	=	positive linear Harmonic Correlation Function
HPSD	=	Harmonic Power Spectral Density
pHPSD	=	positive Harmonic Power Spectral Density
LTI	=	Linear Time Invariant
LTP	=	Linear Time Periodic

## State Space LTI System

$A$	=	diagonal matrix of system poles
$B$	=	control or input matrix
$C$	=	output matrix
$P$	=	matrix of state space eigenvectors
$q$	=	state of the uncoupled system, or modal participation factor

<sup>1</sup> Graduate Assistant, Engineering Physics Department, 534 Engineering Research Building, 1500 Engineering Drive, Madison, WI 53706-1609, AIAA Member, [syang66@wisc.edu](mailto:syang66@wisc.edu).

<sup>2</sup> Assistant Professor, Engineering Physics Department, 535 Engineering Research Building, 1500 Engineering Drive, Madison, WI 53706-1609, AIAA Member, [msallen@engr.wisc.edu](mailto:msallen@engr.wisc.edu).

$u$	=	state space input
$y$	=	state space output
$x$	=	position of laser spot
$r$	=	integer referring to a particular mode
$\psi_r$	=	$r$ th mode shape of the underlying LTI system
$\omega_r$	=	$r$ th natural frequency of the underlying LTI system
$\zeta_r$	=	$r$ th damping ratio of the underlying LTI system
$\lambda_r$	=	$r$ th eigenvalue of the underlying LTI system
<b>LTP system</b>		
$l$	=	integer describing the offset of a harmonic peak for a particular mode
$n$	=	integer giving the order of a harmonic in a Fourier series expansion or an EMP signal
$T_A$	=	fundamental period of the LTP system
$\omega_A$	=	fundamental frequency of the LTP system or scan frequency for CSLDV, $\omega_A = T_A / 2\pi$
$U_n(\omega)$	=	$n$ th harmonic of the EMP input in the frequency domain
$Y_n(\omega)$	=	$n$ th harmonic of the EMP output in the frequency domain
$\mathbf{Y}(\omega)$	=	collection of EMP output signals
$\mathbf{U}(\omega)$	=	collection of EMP input signals
$\mathbf{G}(\omega)$	=	harmonic transfer function matrix
$\bar{\mathbf{C}}_{r,l}$	=	EMP mode vector at the $l$ th harmonic of the $r$ th mode
$C_{r,n}$	=	$n$ th Fourier coefficient for the $r$ th time varying mode shape
$\mathbf{A}_{r,l}$	=	Residue of the $l$ th harmonic of the $r$ th mode in HPSD
$S_{\mathbf{Y}\mathbf{Y}}(\omega)$	=	autospectrum of EMP output, or HPSD
$H_{\mathbf{Y}\mathbf{Y}}(\omega)$	=	pHPSD
$R[n]$	=	linear harmonic correlation function
$R_m[k]$	=	lifted linear harmonic correlation function at the $m$ th point
$\mathbb{R}_m(\omega)$	=	FFT of pHCF for the $m$ th point on the laser path
<b>Res</b> $_{r,m}$	=	residue matrix of the $r$ th mode identified from the lifted pHCF at $m$ th point.
$\chi_{r,l}$	=	modal contribution constant of the $l$ th harmonic for $r$ th mode

## I. Introduction

In continuous-scan laser Doppler vibrometry (CSLDV), the laser spot continuously sweeps over a structure while recording the response along the scan path, reducing the time required to measure the structure's mode shapes. Many researchers have investigated CSLDV since it was first introduced in 1990s [1]. Among them, Ewin, Stanbridge et al. have modeled the operating deflection shape as a continuous polynomial function of the laser spot position. The polynomial coefficients are obtained from the sideband peaks in the spectrum of measured response, and the operating shape can then be reconstructed with these coefficients. This method has been successfully applied with sinusoidal [2], impact [3], and pseudo-random excitation [4]. On the other hand, Allen et al. proposed a lifting approach where the responses at the same location are grouped together to form a set of pseudo transducers along the laser path [5]. The measured spectra from the pseudo transducers are the same as would be obtained with an array of conventional sensors, except that there is a constant time delay between these pseudo sensors, and the sampling rate of each sensor becomes the laser scan frequency. So the natural frequencies higher than the half of the scan frequency will be aliased according the Nyquist-Shannon sampling theorem. The authors applied the lifting method to a free-free beam under impact excitation and the unaliased natural frequencies and mass normalized mode shapes were identified [6]. The advantage of the lifting approach is that it produces a set of spectra that are mathematically equivalent to a collection of frequency response functions at a set of points. Hence, the structure's modes are readily extracted from the measurements using standard software. However, this method is more suitable for structures with low natural frequencies because speckle noise and the mirror inertia limit the maximum practical scan frequency.

All of these methods require that the force exciting the structure be either impulsive or some known, carefully controlled function (e.g. sinusoidal). However, sometimes it is difficult or even impossible to directly measure the dynamic load on a structure, for example, wind turbines or aircraft wings excited by fluctuations in the flow field. CSLDV is especially attractive for these applications because it can provide spatially detailed mode shapes with as few as one single measurement, before the excitation conditions or the structure changing appreciably. In the authors' previous work [7], the measured response using CSLDV was treated as a the output of a linear time periodic (LTP) system, and an output-only methodology was proposed based Wereley's harmonic transfer function (HTF) concept [8]. The HTF, for an LTP system, is equivalent to the transfer function of linear time invariant (LTI) system and was used to define a new type of spectrum, dubbed the harmonic power spectrum (HPSD) which is formed from the CSLDV measurement. The structure's mode shapes, natural frequencies and damping ratios can then be obtained from the HPSD using peak-picking or conventional operational modal analysis curve fitting routines. The method was used to identify several modes of a parked wind turbine blade under wind excitation [7].

While the method presented in [7] has proved effective, the identification procedure is somewhat labor intensive since a multitude of peaks are present in the HPSD for each mode of the system. The resulting mode shapes can also vary depending on which peaks in the HPSD are used to estimate them. On the other hand, the authors' lifting method [5, 6] allowed one to extract a set of mode shapes from CSLDV measurements almost automatically. This work seeks to extend the lifting method to output only measurements. This is accomplished by using the positive harmonic correlation function (pHCF), which is analogous to an impulse response function and can be estimated from the HPSD. The approach used is basically an extension of the positive power spectrum concept, developed by Cauberghe for LTI systems [9], to linear time periodic systems. In Cauberghe's works, the positive correlation function was transformed into a positive power spectrum, which is a FRF-like function that can be treated with conventional curve-fitting routines. That method was extended to LTP systems in [10], revealing that one could obtain similar results with the HPSD or pHPSD, although the latter are more convenient to curve fit. However, both of those spectra contain several peaks for each mode so quite a bit of effort is required to perform system identification. In this work, the pHCF is lifted using the approach in [5, 6] to compute spectra that are analogous to a set of Single-Input Multi-Output (SIMO) frequency response functions, similar to what would be obtained from an array of stationary sensors. The resulting spectrum is much simpler to interpret than the HPSD, and can be curve-fit with virtually any modal parameter identification routine to identify the natural frequencies, damping ratios and mode shapes of the structure.

The rest of this paper is organized as follows. Section II briefly introduces the harmonic power spectrum concept, the harmonic correlation function and the proposed lifting approach. In Section III, the proposed algorithm is demonstrated on a simulated beam and compared with the HPSD and pHPSD methods. In Section IV the algorithm is tested on a real wind turbine under ambient excitation, using measurements from a new long range laser vibrometer, the Remote Sensing Vibrometer (RSV) from PolyTec<sup>®</sup> with a customized mirror system. Section V presents the conclusions.

## II. Theory

### A. Harmonic Transfer Function and Harmonic Power Spectrum

When applying CSLDV with a closed, periodic scan pattern to a LTI structure, the output appears to be from a LTP system. Following the derivation in [7], the equation of motion for the system can be written in uncoupled state space form as,

$$\begin{aligned}\dot{q} &= \Lambda q + P^{-1}Bu \\ y &= CP(t)q\end{aligned}\tag{1}$$

where  $\Lambda$  is a diagonal matrix containing the eigenvalues,  $\lambda_r = -\zeta_r \omega_r + j\omega_r \sqrt{1 - \zeta_r^2}$ , of the system, with  $\zeta_r$  the modal damping ratio and  $\omega_r$  the natural frequency, and  $P$  is a matrix of state space eigenvectors. The only periodic term in the LTP system is the output matrix  $CP(t)$ , which is a row vector containing the shape of each mode of the system at the current time instant. Following the derivation in [7]

this is denoted

$$CP(t) = [\psi_1(x(t)), \dots, \psi_N(x(t)), \psi_1^*(x(t)), \dots, \psi_N^*(x(t))] \quad (2)$$

where  $x(t) = x(t+T_A)$  denotes the position of the LDV measurement point at time  $t$  and  $\psi_r(x)$  denotes the state space mode shape at location  $x$  and in the direction sensed by the laser. The fundamental period of the scan pattern has been denoted  $T_A$  and it is understood that the laser path  $x(t)$  could involve motion in three dimensions.

It is well known that a single frequency input to a LTI system leads to an output at the same frequency. In contrast, the response of a LTP system will be at the input frequency and also at an infinite number of harmonics, each separated by the fundamental frequency  $\omega_A$  of the LTP system,  $\omega_A = T_A / 2\pi$ . The LTP identification strategy makes use of the harmonic transfer function concept [11], which relates the input and output of LTP system by introducing the exponentially modulated periodic (EMP) signal. The EMP signal is composed of the input or output at a collection of frequencies separated by  $\omega_A$ . For example, if the response measured with continuously scanning laser vibrometer is denoted  $y(t)$ , and the scan frequency (fundamental frequency) is  $\omega_A$ , then one could compute the EMP signal  $\mathbf{Y}(\omega)$  by taking the Fourier transform of  $y(t)$  and then shifting the spectrum by  $n\omega_A$ . These steps can actually be combined as follows.

$$Y_n(\omega) = \int_{-\infty}^{\infty} y(t) e^{(-j\omega - jn\omega_A)t} dt \quad (3)$$

The EMP signal is the collection of the frequency shifted copies of  $Y_0(\omega)$ .

$$\mathbf{Y}(\omega) = [\dots Y_{-1}(\omega) Y_0(\omega) Y_1(\omega) \dots]^T \quad (4)$$

Wereley performed a similar operation on the input forces  $u(t)$ , and used the general solution of the state space equation and a harmonic balance approach to relate the input and output with a harmonic transfer function (HTF),  $\mathbf{G}(\omega)$ . Details of this derivation can be found in [8], Chapter 3.

$$\mathbf{Y}(\omega) = \mathbf{G}(\omega)\mathbf{U}(\omega) \quad (5)$$

Notice that the HTF is a matrix even in the case where we only have a single input and a single output, because it relates the response of LTP system at  $\omega$  and its harmonics  $\omega + \omega_A$ ,  $\omega - \omega_A$ , etc... to the input at the same frequencies. In this work we are concerned with the case where the output is measured using a single beam CSLDV and therefore it is a scalar and the input is unknown white noise and potentially applied to many points along the structure.

In [7] the authors showed that the harmonic output autospectrum (HPSD) of the LTP system can be written as follows.

$$S_{\mathbf{Y}\mathbf{Y}}(\omega) = E(\mathbf{Y}(\omega)\mathbf{Y}(\omega)^H) \approx \sum_{r=1}^N \sum_{l=-\infty}^{\infty} \frac{\bar{\mathbf{C}}_{r,l} \mathbf{W}(\omega)_{r,l} \bar{\mathbf{C}}_{r,l}^H}{[j\omega - (\lambda_r - j l \omega_A)][j\omega - (\lambda_r - j l \omega_A)]^H} \quad (6)$$

The equation on the right is an approximation because it neglects cross terms between pairs of modes where one mode is resonant and the other is not. For a structure under uncorrelated random white noise input,  $\mathbf{W}(\omega)_{r,l}$  is a scalar related to the net excitation of the  $r$ th mode and does not depend on  $l$ , so it is written as  $\mathbf{W}(\omega)_r$  from this point forward [7]. The elements in the vectors  $\bar{\mathbf{C}}_{r,l}$  are not the usual mode shapes (i.e. the amplitudes of motion at various points on the structure) but are Fourier coefficients that describe the  $r$ th time varying mode shape and are defined below.

$$C(t)\psi_r = \psi_r(x(t)) = \sum_{n=-\infty}^{\infty} C_{r,n} e^{jn\omega_A t} \quad (7)$$

$$\bar{\mathbf{C}}_{r,l} = [\dots C_{r,-1-l} \quad C_{r,-l} \quad C_{r,1-l} \quad \dots]^T$$

Of course, the structure's  $r$ th mode shape is time invariant but it appears to be time varying in the CSLDV measurement because the laser spot is continuously moving.

The HPSD has the same form as the output autospectrum of an LTI system; it is a sum of modal contributions. However, the time varying mode shapes of the system give rise to peaks in the CSLDV response near each natural frequency  $\omega_r$ , and also at the frequencies  $\omega_r \pm l\omega_A$  for any integer  $l$ . Hence one can obtain an estimate of each mode vector,  $\bar{\mathbf{C}}_{r,l}$ , from a number of different peaks, although the terms in each vector  $\bar{\mathbf{C}}_{r,l}$  contain the Fourier coefficients but shifted at different locations as explained in [7]. For example, the fundamental term in the Fourier series,  $C_{r,0}$  is found in the center of  $\bar{\mathbf{C}}_{r,0}$ , but that term appears  $l$  terms below the center in  $\bar{\mathbf{C}}_{r,l}$ .

Eq. (6) can be decomposed into a convenient form by partial fraction expansion. This results in terms that are resonant at both the stable poles  $(\lambda_r - jl\omega_A)$ ,  $(\lambda_r - jl\omega_A)^*$ , which have negative real parts, and unstable poles  $-(\lambda_r - jl\omega_A)$ ,  $-(\lambda_r - jl\omega_A)^*$ . The HPSD then can be written as follows,

$$S_{YY}(\omega) \approx \sum_{r=1}^{N/2} \sum_{l=-\infty}^{\infty} \frac{\mathbf{A}_{r,l}}{[j\omega - (\lambda_r - jl\omega_A)]} + \frac{\mathbf{A}_{r,l}^*}{[j\omega - (\lambda_r - jl\omega_A)^*]} + \frac{\mathbf{A}_{r,l}^*}{[-j\omega - (\lambda_r - jl\omega_A)]} + \frac{\mathbf{A}_{r,l}}{[-j\omega - (\lambda_r - jl\omega_A)^*]} \quad (8)$$

where the residue matrix at the  $l$ th harmonic for the  $r$ th mode is defined as follows.

$$\mathbf{A}_{r,l} = \frac{\bar{\mathbf{C}}_{r,l} \mathbf{W}(\omega) \bar{\mathbf{C}}_{r,l}^H}{\zeta_r \omega_r} \quad (9)$$

Hence, one can extract the Fourier coefficients of the time varying mode shapes by curve fitting the measured HPSD to a standard modal model with both stable and unstable poles at each peak. The time varying mode shapes can then be reconstructed with the identified Fourier coefficient vectors using Eq. (7), and since the laser scan path is known this can be used to determine the structure's mode shapes along the scan path. This approach was used in [7] and found to work quite well, although there are potentially many peaks to be fit in the power spectrum even if the structure has only a few modes.

## B. Positive Harmonic Linear Correlation and Positive Harmonic Power Spectrum

The HPSD in Eq. (8) includes each of the system's poles twice, one set having stable poles and the other having unstable poles, so one must use a curve fitting routine that is specialized to OMA measurements (most common curve fitting routines are derived for frequency response function measurements where the unstable poles are not needed). The equivalent issue for the case of LTI measurements has been addressed in conventional operational modal analysis using the positive power spectrum [9]. Allen et al. extended this concept to LTP systems, defining the positive Harmonic Power Spectrum [10].

First, each block of the exponentially modulated time signal is zero-padded to twice its length and the HPSD is computed. The linear harmonic correlation function is the one side inverse DFT of the HPSD in Eq (8), as shown below,

$$R[n] = \sum_{r=1}^{N/2} \sum_{l=-\infty}^{\infty} \mathbf{A}_{r,l} e^{(\lambda_r - jl\omega_A)nT_s} + \mathbf{A}_{r,l}^* e^{(\lambda_r - jl\omega_A)^* nT_s} + \mathbf{A}_{r,l}^* e^{-(\lambda_r - jl\omega_A)(n-N_s)T_s} + \mathbf{A}_{r,l} e^{-(\lambda_r - jl\omega_A)^*(n-N_s)T_s}, \quad 0 \leq n < N_s \quad (10)$$

where  $T_s$  is the laser sampling period, and  $N_s$  is number of samples in the HPSD. When  $n$  is small, the first two terms in Eq. (10) dominate the response, so the harmonic correlation function takes on the form of an impulse response function that has only stable poles. However, as  $n$  increases, the first two terms damp out and the last two terms with positive real parts become dominant. Often the terms for the last  $N/2$  samples are shifted to the left and used as an estimate of the impulse response function for negative time lags. However, Cauberghe suggested instead that a rectangular window be used to delete the part of the HCF that corresponds to negative time lags. This leaves only the pHCF, which is analogous to a

one-sided impulse response as might be found in a hammer modal test. Then, the pHPSD,  $H_{\text{YY}}(\omega)$ , is found by computing the FFT of the pHCF, and the result is a spectrum that contains only the positively damped poles.

$$H_{\text{YY}}(\omega) \approx \sum_{r=1}^{N/2} \sum_{l=-\infty}^{\infty} \frac{\mathbf{A}_{r,l}}{[\mathbf{j}\omega - (\lambda_r - \mathbf{j}l\omega_A)]} + \frac{\mathbf{A}_{r,l}^*}{[\mathbf{j}\omega - (\lambda_r - \mathbf{j}l\omega_A)^*]} \quad (11)$$

The pHPSD has the same mathematical form as a frequency response function and can be curve fit using standard methods. This pHPSD approach was applied to data from an LTP system in [10].

### C. Lifting the Positive Harmonic Correlation

This work explores a different analysis procedure, which dramatically simplifies the post processing of the CSLDV measurements. The pHCF is similar to the impulse response of the system. If there are exactly  $N_A$  samples per scan period then one can define  $N_A$  points on the structure, at  $m$ th point samples have been acquired at time instants  $mT_s + kT_A$ . The response of the  $m$ th point at its  $k$ th time instant can then be obtained from the first two terms in Eq. (10) as

$$R_m[k] \approx \sum_{r=1}^{N/2} \sum_{l=-\infty}^{\infty} \mathbf{A}_{r,l} e^{(\lambda_r - \mathbf{j}l\omega_A)mT_s} e^{\lambda_r kT_A} + \mathbf{A}_{r,l}^* e^{(\lambda_r - \mathbf{j}l\omega_A)^* mT_s} e^{\lambda_r^* kT_A} \quad (12)$$

Lifted responses exist for  $m = 0 \dots (N_A - 1)$  and each lifted response contains one sample at each instant  $kT_A$  over the span of the measurement. This resampling causes the eigenvalues  $\lambda_r - \mathbf{j}l\omega_A$  to collapse to a single frequency and hence the lifted response contains only one exponential term per mode of the underlying LTI system. The number of points,  $N_A$ , obtained per scan cycle (and hence the number of lifted responses) is related to the sample increment of the laser,  $T_s$ , and the scan period  $T_A$  by  $T_A = N_A T_s$ . The FFT of the lifted linear correlation function at the  $m$ th point then becomes

$$\mathbb{R}_m(\omega) = \sum_{r=1}^N \frac{\mathbf{Res}_{r,m}}{i\omega - \lambda_r} + \frac{\mathbf{Res}_{r,m}^*}{i\omega - \lambda_r^*} \quad (13)$$

$$\mathbf{Res}_{r,m} = \sum_{l=-\infty}^{\infty} \mathbf{A}_{r,l} e^{(\lambda_r - \mathbf{j}l\omega_A)mT_s}$$

This expression has the same mathematical form as a frequency response function with a single resonance at  $\omega \approx \text{Imag}(\lambda_r)$  from each mode. Note that some modes may be aliased so they would appear to occur at  $0 < \omega < \omega_A/2$ . When this occurs the true (unaliased)  $\lambda_r$  can be found by adding the correct integer multiple of  $\omega_A$ , as discussed in [5, 6]. Hence, the multitude of peaks for each integer  $l$  in eq. (11) have collapsed onto a single frequency  $\omega$  between  $[0, \omega_A/2]$ . We can then use a least square approach to recover the mode vector from the identified residue at each resonance.

Suppose  $n = -p \dots p$  is used to modulate the EMP signal, and that significant harmonics are present for the  $r$ th mode for  $l = -q \dots q$  in HPSD (one must select  $p > q$  to obtain meaningful results). Then the  $r$ th identified residue at the  $m$ th measurement point  $\mathbf{Res}_{r,m}$  is a column vector of  $(2p+1)$  elements that sums

the contributions of each sideband  $\sum_{l=-q}^q \mathbf{A}_{r,l} e^{(\lambda_r - \mathbf{j}l\omega_A)mT_s}$ . There are  $N_A$  measurement point along the scan path, therefore the residue for the  $r$ th mode has dimensions  $(2p+1) \times N_A$ , as follows.

$$\begin{aligned}
\mathbf{Res}_r &= \begin{bmatrix} \sum_{l=-q}^q \mathbf{A}_{r,l} & \sum_{l=-q}^q \mathbf{A}_{r,l} e^{(\lambda_r - j l \omega_A) T_s} & \dots & \sum_{l=-q}^q \mathbf{A}_{r,l} e^{(\lambda_r - j l \omega_A) (N_A - 1) T_s} \end{bmatrix}_{(2p+1) \times N_A} \\
&= \begin{bmatrix} \bar{\mathbf{C}}_{r,-q} \chi_{r,-q} & \dots & \bar{\mathbf{C}}_{r,q} \chi_{r,q} \end{bmatrix}_{(2p+1) \times (2q+1)} \begin{bmatrix} 1 & e^{(\lambda_r + j q \omega_A) T_s} & \dots & e^{(\lambda_r + j q \omega_A) N_A T_s} \\ \vdots & \vdots & \vdots & \vdots \\ 1 & e^{(\lambda_r - j q \omega_A) T_s} & \dots & e^{(\lambda_r - j q \omega_A) N_A T_s} \end{bmatrix}_{(2q+1) \times N_A} \\
&= \mathbf{X}_r \mathbf{E}_r
\end{aligned} \tag{14}$$

Where  $\chi_{r,q}$  is a constant scalar that represents  $\mathbf{W}(\omega)_r C_{r,-q}^H / (\zeta_r \omega_r)$ . A least squares problem can then be formed to obtain the  $\mathbf{X}_r = [\bar{\mathbf{C}}_{r,-q} \chi_{r,-q} \dots \bar{\mathbf{C}}_{r,q} \chi_{r,q}]$  matrix, as  $\mathbf{X}_r = \mathbf{Res}_r \mathbf{E}_r^H (\mathbf{E}_r \mathbf{E}_r^H)^{-1}$ , and then singular value decomposition can be used to extract  $\bar{\mathbf{C}}_{r,0}$  after shifting each column in  $\mathbf{X}_r$  according to the position of each sideband with respect to the unaliased natural frequency, as was elaborated in [7]. Then the mode shapes can be reconstructed from the Fourier coefficients in  $\bar{\mathbf{C}}_{r,0}$  using eq. (7).

#### D. Signal Processing Procedure

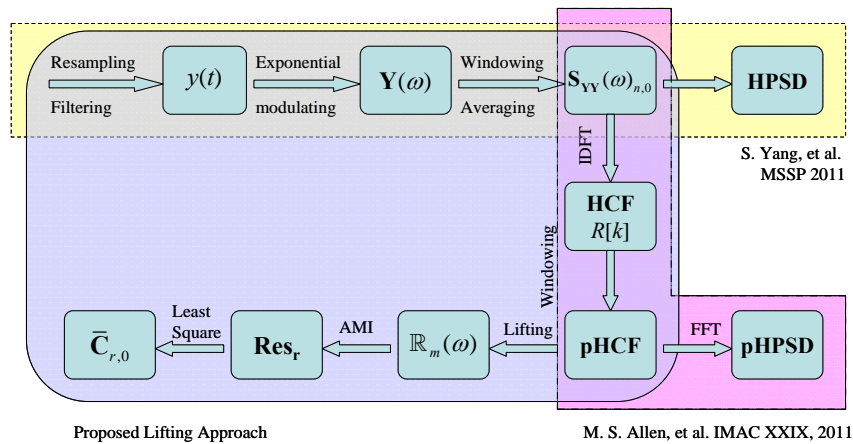


**Figure 1. Output only algorithms for CSLDV**

Figure 1 outlines the signal processing procedure for the proposed CSLDV method with lifting and shows how the proposed approach is related to the authors' previous output-only methods for CSLDV and linear time periodic systems. The steps involved in the proposed algorithm are explained in more detail below

1. Record the response,  $y(t)$ , of an LTI system to a white noise random input using CSLDV with a periodic scan path.
2. Resample the response  $y(t)$  according to the scan frequency  $\omega_A$  such that there are precisely  $N_A$  samples per scanning period. A method for doing this is discussed in [5].
3. Build the EMP signals with  $n=-p \dots p$  in time domain by defining the  $n$ th modulated time signal as  $y_n(t) = y(t) e^{-jn\omega_A t}$
4. Break these EMP signals into sub blocks, apply a Hanning window with overlap, if desired, zero-pad each block to twice its length and compute the discrete Fourier transform. Compute the primary column of the HPSD matrix using the usual technique (e.g.  $S_{YY}(\omega)_{n,0} = E(\mathbf{Y}(\omega) \mathbf{Y}_0(\omega)^H)$  where the expectation operator denotes the average over all available estimates of the  $\mathbf{Y}(\omega)$ ).

5. Take inverse FFT of the HPSD to obtain the linear HCF. Use a rectangular window to delete the negative part of the HCF.
6. Lift the pHCF by grouping the responses at the same location along the laser path according to Eq. (12) and then take the FFT to obtain a spectrum that is described by the modal model in Eq. (13).
7. Identify the eigenvalues of the structure and the corresponding mode shapes using a modal parameter identification routine such as AMI [12], or a simple approach such as peak picking could be used if the system is very lightly damped.
8. The natural frequencies of the structure can be obtained from the identified eigenvalues using a variant on the unaliasing algorithm described in [5].
9. The identified residue is used to form the least square problem in Eq. (14). After shifting to align the Fourier coefficients, the singular value decomposition method described in [7] is used to find the best estimate of the Fourier coefficient vector  $\bar{C}_{r,0}$ .
10. The  $r$ th mode shape can be reconstructed from the Fourier coefficient vector using Eq. (7). The time varying shape  $C(t)\psi_r$  is plotted versus the laser scan path to obtain the mode shapes of the underlying LTI system.

Notice that all of these steps except for the identification in step 7 are readily automated, so the user only need be concerned with interpreting the lifted spectrum and extracting any modes that are present. These steps are far simpler using the lifted spectrum than they are using the full HPSD, as will be shown in the examples that follow.

### III. Simulation Results

The proposed algorithm was first evaluated using simulated measurements from a free-free beam. This provided flexibility in varying the parameters used to test the beam and the accuracy of the method could be assessed since the exact solution is available. Table 1 lists the physical parameters of the beam that simulates a real beam tested in [6]. The simulated response is also processed with the HPSD and pHPSD algorithm, and the results are evaluated and the advantages and disadvantages of each method are discussed.

**Table 1: Parameters for the simulated CSLDV test**

Beam geometry	L 971.6 mm × H 25.4 mm × W 3.2 mm
Density	2710 kg/m <sup>3</sup>
Elastic modulus	66 GPa
Laser scan frequency	128 Hz
Laser sampling frequency	10240 Hz
Simulated duration	488 s

The first 5 bending modes with 0.5% modal damping are used to construct the mass, damping and stiffness matrices by means of the Ritz method [13]. The response of the beam under random excitation is obtained using the '*lsim*' function in Matlab with the simulated model. The mode shape is varied periodically to simulate a case where a laser scans a line pattern for 488s at the frequency of 128Hz with the sampling frequency of 10,240Hz; these parameters are more than feasible with the laser vibrometer used in [5]. These acquisition settings result in 80 pseudo measurement points along the scan path.

The simulated time history is then used to built the EMP output signal according to step 3 with  $n=-10 \dots 10$ . Each of the 21 exponentially modulated time histories are then divided into 6.4s sub-blocks with 50% overlap and a Hanning window is applied. Each block is then zero-padded to twice its original length, and the auto and cross spectra between the modulated signals and the original time history (unmodulated history) are computed and averaged over 150 blocks to obtain the primary column of the HPSD,  $S_{YY}(\omega)_{n,0}$ . The resulting HPSD is shown in Figure 2.

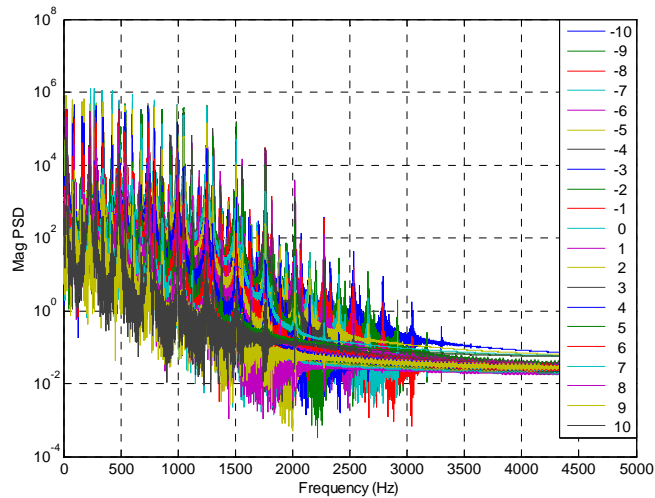


**Figure 2. Primary column of the HPSD  $S_{YY}(\omega)_{n,0}$  for the simulated free-free beam. The index,  $n$ , ranges from -10 to 10 as shown in the legend.**

There are several harmonics in the spectra up to 3000Hz, due to each of the beam's 5 modes and all of their sidebands according Eq. (6). The sidebands of each mode also spread over a wide range of frequency since the sidebands are separated by the 128Hz scan frequency. In addition, folding happens when any of the sidebands reaches the negative plane, further complicating the modal identification. In [7] the authors described a semi-automatic procedure that can be used to locate the sidebands of each mode. An estimate of the mode vector can then be obtained from each peak using peak-picking. This procedure was used and the physical mode shape was reconstructed, although the procedure did require quite a bit of user input to discard peaks where the response was noisy and the mode shapes were found to vary depending on which peaks were included in the peak picking. The identified natural frequencies and damping ratios are listed in Table 2 along with the modal assurance criterion (MAC) between the identified shapes and the true mode shapes. The damping ratios were obtained by curve fitting a few of the dominant peaks in the HPSD.

Next the pHPSD and new lifting method were used. This was accomplished by applying a two sided inverse DFT to the spectrum  $S_{YY}(\omega)_{n,0}$  to obtain the corresponding linear harmonic correlation function. A rectangular window was then used to zero out the negative HCF. The pHCF has the same length as the original 6.4s measurement blocks since the harmonic power spectrum was computed with linear correlation. Hence the pHCF has 80 pseudo measurement points in each scan cycle as well. The responses at the same measurement point are then grouped to form a single-input multi-output system that has 80 pseudo sensors for each of the 21 pHCF, for a total of 1680 outputs. Figure 3 shows the composite response of the lifted pHCF, which is the average over all 1680 measurements. As mentioned previously, the lifting method aliases all of the sidebands of each mode to frequencies between 0 and  $\omega_A/2$ . The lifted response contains only one peak for each mode and when the measurements from the various pseudo-points are averaged the resulting spectrum is very clean. The AMI modal identification routine [12] was able to process this set of measurements semi-automatically to identify the natural frequencies and damping ratios. The curve fit to the measurements is shown in Figure 3 with a dotted line. The red line shows the error between the fitted response and original data, where we can observe that the fitting is actually very accurate. It is important to note that AMI treats the entire 1680-output set of measurements; plots of the average spectra such as that shown here are used only for visualization purposes. Hence, the residue vector returned by AMI had 1680 elements. These were processed according to step 8 and an optimal estimate of the Fourier coefficient vector was then extracted and used to reconstruct the physical mode shape by plotting the time varying shapes versus the laser scan path. Figure 4 shows the mode shape extracted for the first mode at the 80 pseudo measurement points (red circles) and compares it with the analytical first bending mode. The MAC values between all of the identified mode vectors and the analytical shapes are given in Table 2.

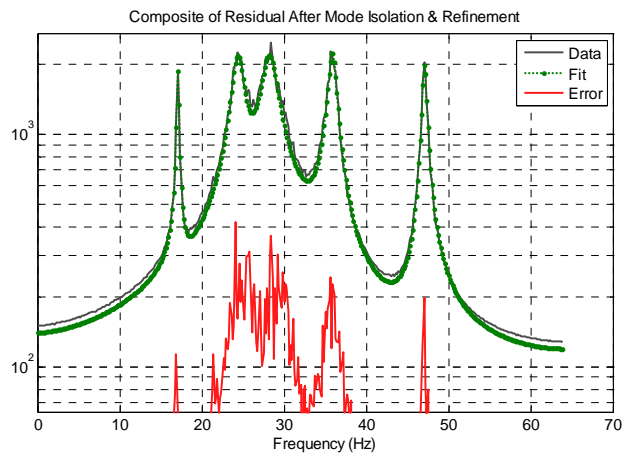


**Figure 3: Lifted pHCF and AMI curve fitting**

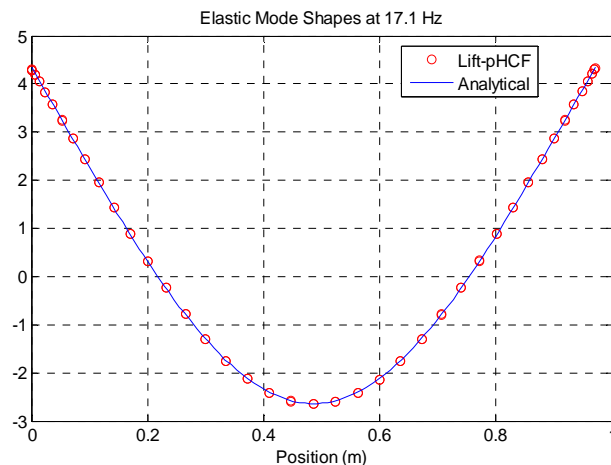


**Figure 4: First bending mode obtained via lift pHCF**

In order to make the comparison complete, the pHPSD method described in [10], which uses the pHPSD in place of the HPSD, was also employed. Recall that the pHPSD is the FFT of the un-lifted pHCF [10]. The pHPSD are similar in appearance to the HPSD in Figure 2 and the identification procedure used here was identical to that described earlier for the HPSD. The primary difference between the pHPSD and HPSD is that the latter is a squared spectrum and hence does not capture the evolution of each mode's phase near resonance. Hence, the HPSD requires a specialized modal parameter modal identification routine while virtually any method can be applied to the pHPSD. The modal parameters extracted from pHPSD are listed in Table 2.

Table 2 compares the identified natural frequencies and damping ratios from the three algorithms with the exact solution. The mode shapes obtained with each method are compared using the MAC between the identified shapes and the true analytical shapes. We can see that the natural frequencies from the three methods are almost identical to the exact values, and the MAC values are greater than 0.99 for all of the modes. The identified damping for the first mode shows significant error, most likely due to distortion caused by the Hanning window [14].

The HPSD, pHPSD and the lifting approach all have very similar accuracy for this example. However, the lifting approach provides a much simpler user interface that greatly reduces the effort required in modal identification. Moreover, the lifting algorithm might also be advantageous if the structure of interest contained modes with close natural frequencies, where MIMO measurements are needed to determine the number of modes present and to identify their parameters.

**Table 2. Comparison of identified mode from different method**

Mode	Analytical		HPSD			pHCF-liftng			pHPSD		
	Frequency (Hz)	Damping (%)	Frequency (Hz)	Damping (%)	MAC	Frequency (Hz)	Damping (%)	MAC	Frequency (Hz)	Damping (%)	MAC
1	17.06	0.5	17.06	0.73	1.0000	17.07	0.66	1.0000	17.08	0.73	0.9998
2	47.04	0.5	47.02	0.57	0.9996	47.08	0.57	1.0000	46.98	0.55	1.0000
3	92.21	0.5	92.16	0.54	0.9997	92.12	0.55	1.0000	92.06	0.55	0.9999
4	152.42	0.5	152.44	0.53	0.9996	152.36	0.49	0.9965	152.42	0.53	0.9927
5	227.70	0.5	227.78	0.48	0.9979	227.79	0.43	0.9952	227.41	0.48	0.9949

#### IV. Application to Wind Turbine Blade using Remote Sensing Vibrometer

The proposed method was then used to identify the modes of a wind turbine blade mounted on the tower, as depicted in Figure 5. The wind turbine is the same as in [7] except with a different set of blades installed. During the tests, the turbine rotor was locked to prevent rotation, and the blade of interest was pitched so that the laser was nominally perpendicular to the chord of the blade (i.e. measuring in the flapwise direction). A prototype of Polytec's new Remote Sensing Vibrometer was used in this work, which incorporates a larger wavelength laser (1550 nm) and higher laser power (10 mW) than previous LDVs. This laser is designed for long standoff distances and hence was able to acquire reasonable measurements without any surface treatment. The standoff distance from the vibrometer to the turbine blade was 77m. (In the authors' prior work [7], a Polytec PSV-400 (633nm laser) vibrometer was used and it was noted that reasonable measurements could not be obtained at that distance unless retro-reflective tape was applied along the length of the scan area.) A customized x-y mirror system was used to redirect the laser of the RSV to scan over as much of the 4.5m long blade as was possible. The blade was excited purely by the wind, whose maximum speed was about 9m/s during the tests.

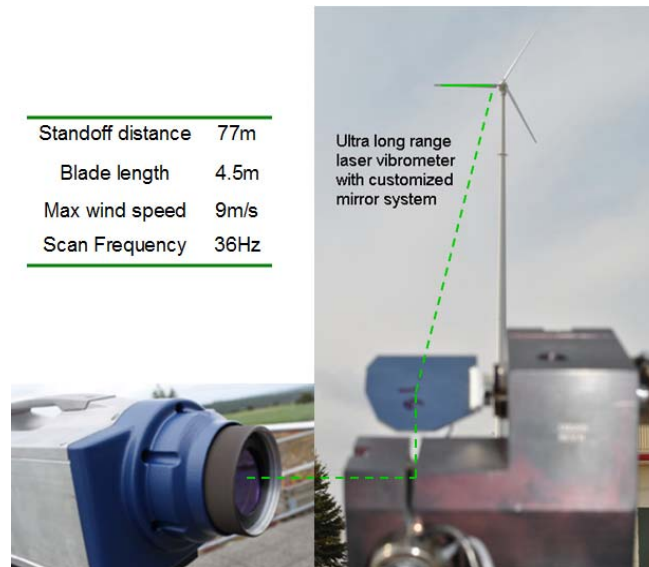


**Figure 5. Schematic of experimental setup.** The photograph on the left shows a generic photo of an RSV vibrometer by Polytec©. The vibrometer used was a prototype with nominally identical specifications.

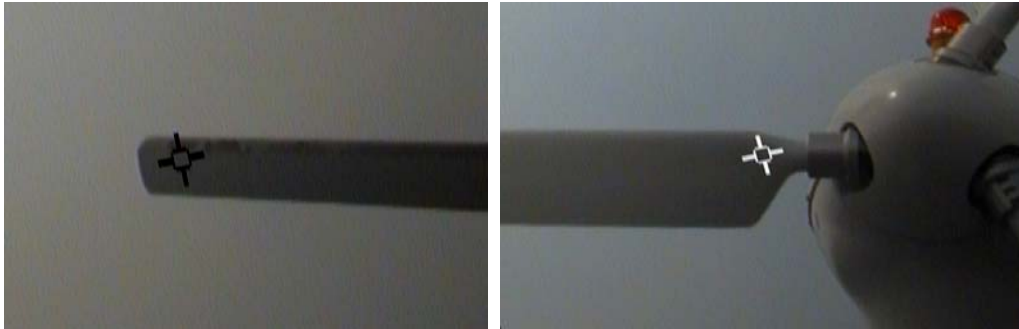


**Figure 6. Photographs showing the position of the CSLDV measurement point at the extremes of its travel. The CSLDV scan path was a line connecting these two points.**

The laser was scanned a line over the blade for 400 seconds with a scan frequency of 36Hz and a sampling frequency of 2560Hz. The laser was not visible, and there was no guide laser in the prototype, so the scan path was defined by determining what voltages to apply to the mirror system to position the laser at the tip and root of the beam as shown in Figure 6. These voltages were then used to define a scan path that corresponded to a line between these two points. This procedure results in far less uncertainty in the position of the measurement points than that used in the authors' previous work [7]. Figure 7 shows the time signal over a few scan cycles (the whole time signal would have the appearance of random noise due to the random nature of the input). The signal is dominated by a 36Hz frequency; however there are clearly several frequencies present in the response, presumably due to the vibration modes of the turbine.

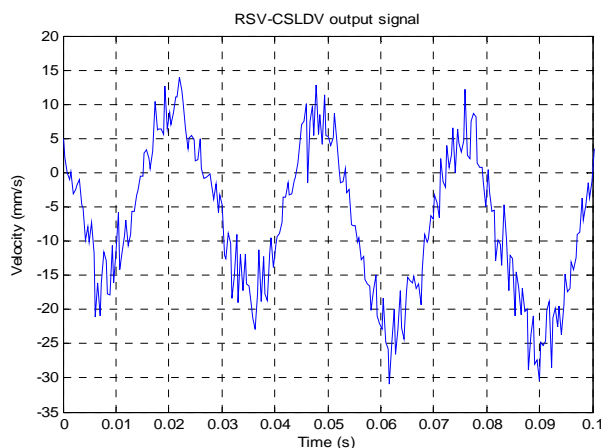


**Figure 7: RSV-CSLDV output signal under random excitation (36Hz scan frequency)**

The whole measured time history was resampled at 2592Hz to generate 72 samples per scan cycle. The resampled signal was low pass filtered and the frequency component corresponding to the 36Hz scan frequency was deleted since it is dominated by speckle noise. The resampled signal was then exponentially modulated with harmonics  $n = -3 \dots 3$ , resulting in 7 modulated time histories. Each of these modulated signals was decomposed into 25.6s sub-blocks with 50% overlap and a Hanning window was applied to each of the 31 blocks. A HPSD of dimensions  $[7 \times 65537]$ , where 65537 is the number of frequency lines, was then obtained as described previously. The pHCF was then obtained using the inverse FFT and rectangular window. Figure 8 presents positive HCF generated from  $S_{YY}(\omega)_{0,0}$ . The pHCF has the appearance of a standard impulse response function with a dominant low frequency mode which persists for more than 20s, and several higher frequency components that disappear after about 10s.

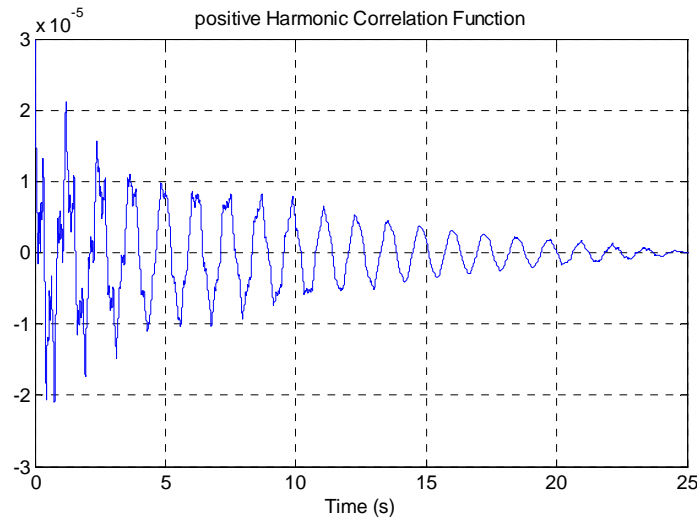


**Figure 8:** pHCF,  $R[n]$ , generated from  $S_{YY}(\omega)_{0,0}$

The pHCF was then lifted and a SIMO system was formed. Figure 9 shows the average of the lifted responses (solid grey line), and the average of the AMI curve fit (dots). Only two peaks are prominent in the plot, but a closer inspection reveals a few other peaks. Specifically, the residual (red line) shows two peaks at 12.3 and 13.3 Hz. These peaks, which are only barely visible in the average spectrum, are actually fairly prominent in the subtraction residual and a mode was identified near each of these peaks. Similarly, there appear to be other close modes near 3.3 Hz, and this is to be expected as three first blade bending modes typically appear at three close frequencies for turbines such as this. A mode was fit to the strongest peak at 3.33 Hz and then natural frequencies and damping ratios of each identified mode are reported in Table 3. Other modes could be fit near 3.3 Hz as well, but it was difficult to be sure that they were meaningful so they are not reported. In any event, measurements would be needed on each blade to obtain meaningful estimates of the various first blade bending modes, as they tend to differ primarily in the relative amplitudes of the three blades.

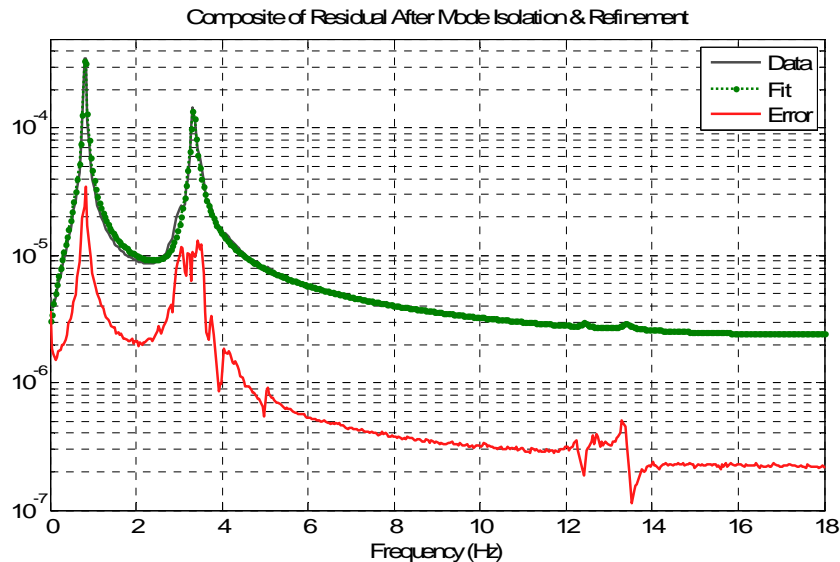


**Figure 9:** Average of the spectrum  $\mathbb{R}_m(\omega)$  of the lifted response, AMI fit and the difference between the two.

The mode shapes were reconstructed from the Fourier coefficients that were identified using eq. (14) and they are shown in Figure 10. The real and imaginary parts of the mode shapes are shown, as AMI fits

a complex mode model to the measurements. However, a lightly damped structure such as this is expected to have real modes so the imaginary parts most likely arise due to inaccuracy in the measurements. They are very small for the first two modes and reasonably small for modes 3 and 4 considering that the response of those modes was two orders of magnitude lower than the dominant mode. The blade appears to move as a rigid body in the first mode, at 0.81Hz, suggesting that this mode primarily involves bending of the tower. The mode at 3.33Hz appears to be the first flap-wise bending mode of the blade. The 0.81 and 3.33 Hz modes both have very small imaginary parts and the shape estimated as the laser spot moved from root to tip agrees very well with the shape estimated as laser spot returned from tip to root, suggesting that the shape is quite accurate. The third and fourth identified frequencies are second bending modes of the blade. These modes have relatively larger imaginary parts but the root-tip and tip-root shapes are quite consistent again suggesting that they have been accurately identified.

**Table 3: Modes identified from the lifted response**

Mode	Natural frequency	Damping
Tower Bending	0.81Hz	1.61%
Flap Wise Bending 1	3.33Hz	1.52%
Flap Wise Bending 2	12.42Hz	0.44%
	13.41Hz	0.70%

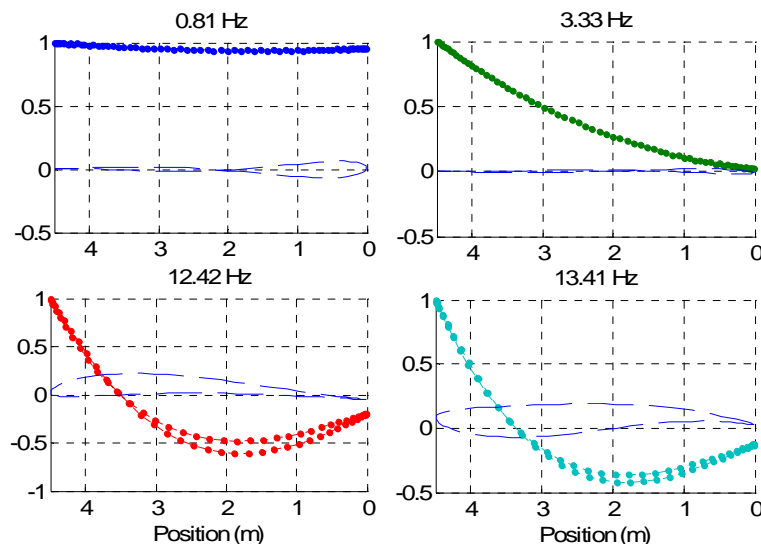


**Figure 10: Real (dots) and imaginary parts (dashed-line) of the mode shapes identified from the CSLDV measurements.**

For comparison purposes, a standard OMA test was also performed and used to estimate the blade's mode shapes. For this test, a patch of retro-reflective tape was applied to the tip of the blade and a PSV-400 LDV was directed towards this point and used as a reference. The RSV laser was then positioned sequentially at five different points along the length of the blade. The positions of the points were determined by measuring the angle of the RSV laser head and using the known length of the blade. The auto and cross spectra between the two lasers was then used to determine the natural frequencies and modes shapes of the turbine from these ten spectra (five autospectra for the reference and five cross spectra between the RSV and PSV-400). The resulting mode shapes are shown in Figure 11. Three different mode shapes were extracted near 3.3 Hz, but, as was discussed previously, there is little evidence that the additional modes are meaningful. Similarly, a third second blade bending mode was identified at 13.0 Hz.

It is informative to compare these results with the CSLDV results. First, one should note that the standard OMA approach required a second laser adding tens of thousands of dollars to the cost of the equipment needed. Second, the standard OMA test required acquisition of five time histories, which

would nominally increase the measurement time by a factor of five. However, since time was limited a smaller number of averages were used for the standard OMA test, and each one of these records was acquired in 5.3 minutes resulting in a total test time of 26.5min for standard OMA and 6.7 min for CSLDV. Third, the measurements obtained by standard OMA agree fairly well qualitatively with those obtained by CSLDV, but there are several points which appear to be questionable. This could possibly be explained by the fact that the wind conditions may have changed from one point to the next, or the reflectivity of the blade surface may have been inferior at some points leading to increased noise. In any event there is little that can be done to assess the reliability of each measurement point without repeating the test. Fourth, the mode shapes obtained by classical OMA seem to be far less detailed than those obtained by CSLDV, On the other hand, because speckle noise was reduced in the standard OMA test, two additional peaks were visible in the spectrum at 4.06 and 5.03 Hz. The second tower bending mode is thought to reside near these frequencies so these shapes are thought to reflect the motion of the blades in the second tower bending mode(s). Since these frequencies are close to the first blade bending mode, it is not surprising that the blades have essentially the same deformation shape as they do in the first bending modes. Although this tower mode was weakly excited its presence could be detected in the standard OMA measurements, while it was buried by speckle noise and the aliased contributions of the dominant modes in the CSLDV measurement.

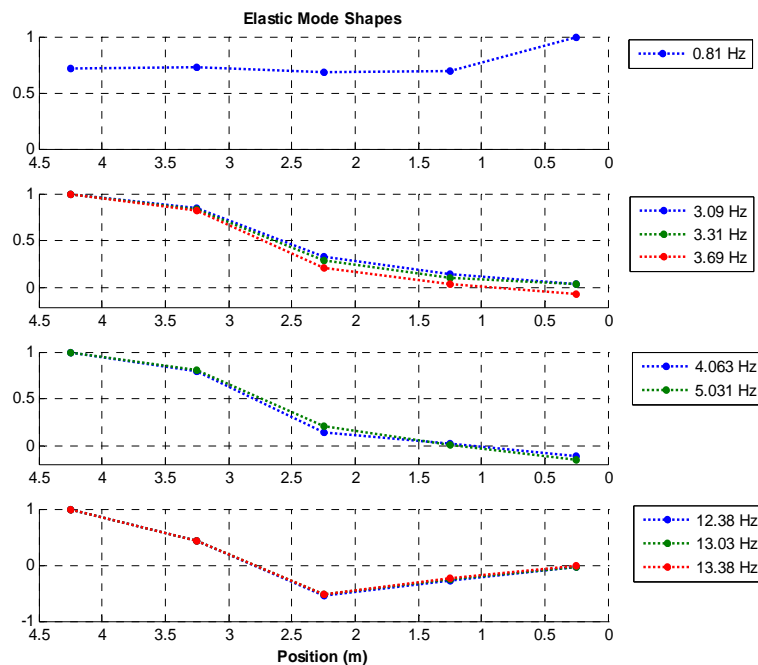


Figure 11: Mode shapes at five points obtained using a standard OMA technique with a second laser serving as a reference.

## V. Conclusion

This paper combined output only continuous-scan laser Doppler vibrometry with a lifting approach, simplifying the post processing required to extract the mode shapes from CSLDV measurements. As with conventional OMA, the method assumes that the forces exciting the system are random, white and that they sufficiently excite all of the modes of interest. The measured CSLDV signal is exponentially modulated to estimate the harmonic power spectrum, and the theoretical development reveals that each mode then appears at several peaks in the HPSD. An inverse FFT is then performed on the HPSD to obtain the harmonic correlation function. The positive HCFs are then lifted and arranged to form a single input multiple output system. A conventional model identification routine such as AMI can then be used to extract modal parameters from the lifted responses. The identified residues have a more complicated definition than they did in [5], but a least squares problem is readily formulated to extract the Fourier coefficients of the mode shapes from the identified residue vectors. The mode shapes can then be

reconstructed by plotting the time varying shapes versus the laser path.

The proposed method was first applied to simulated measurements from a free-free beam. The modes extracted from the measurements using the HPSD (method in [7]), pHPSD (method in [10]) and the new lifting approach showed that similar results could be obtained with any of the approaches. However, the lifting approach provides a much simpler user interface that greatly reduced the effort required to extract the modal parameters.

The methodology presented here was further explored by applying it to measure the modes of a parked wind turbine with a new long range vibrometer called the remote sensing vibrometer (RSV). In this application the RSV laser was capable of extracting accurate measurements at a large standoff distance (77 meters) without any surface treatment. The authors' previous work used a standard vibrometer and reasonable measurements were not possible unless retro-reflective tape was first applied to the surface of the blade. Furthermore, the speckle noise in the measurements with the RSV was relatively small so, high scan frequencies were possible increasing the attractiveness of the lifting approach. This is quite remarkable, since at a 36 Hz scan frequency the peak surface velocity of the laser spot was about 500 m/s. Hence, it appears that this methodology would be feasible for large wind turbines where the natural frequencies are lower and hence the time required to obtain operational modal analysis data can often be excessive.

For the results presented in this work, a single 6.7-min. CSLDV time history was used to extract several modes of vibration including mode shapes with good repeatability. During the post-processing it was noted that it would have been preferable to have a longer time history, since the number of averages (31) was somewhat marginal. However, the measurements were still adequate to obtain qualitatively reasonable results for the first several modes of the turbine. The CSLDV results were compared with those from a standard OMA test using a second laser as a reference, revealing the relative merits of the two approaches. When two lasers are available, the authors recommend a blended approach where CSLDV is used to capture spatially detailed shapes over critical surfaces and point measurements are used to verify the CSLDV results, capture additional discrete points of interest and to identify weakly excited modes.

### Acknowledgements

This material is based on work supported by the National Science Foundation under Grant No. CMMI-0969224. The authors wish to thank Renewegy LLC, [www.renewegy.com](http://www.renewegy.com), for making their facilities available for the testing described here. The authors also wish to thank Vikrant Palan and Arend von der Lieth from PolyTec<sup>®</sup> for their assistance with the Remote Sensing Vibrometer.

### References

- [1] P. Sriram, J. I. Craig, and S. Hanagud, "Scanning laser Doppler vibrometer for modal testing," *International Journal of Analytical and Experimental Modal Analysis*, vol. 5, pp. 155-167, 1990.
- [2] A. B. Stanbridge and D. J. Ewins, "Modal testing using a scanning laser Doppler vibrometer," *Mechanical Systems and Signal Processing*, vol. 13, pp. 255-70, 1999.
- [3] R. Ribichini, D. Di Maio, A. B. Stanbridge, and D. J. Ewins, "Impact Testing With a Continuously-Scanning LDV," in *26th International Modal Analysis Conference (IMAC XXVI)* Orlando, Florida, 2008.
- [4] D. D. Maio, G. Carloni, and D. J. Ewins, "Simulation and validation of ODS measurements made using a Continuous SLDV method on a beam excited by a pseudo random signal," in *28th International Modal Analysis Conference (IMAC XXVIII)* Jacksonville, Florida, 2010.
- [5] M. S. Allen and M. W. Sracic, "A New Method for Processing Impact Excited Continuous-Scan Laser Doppler Vibrometer Measurements," *Mechanical Systems and Signal Processing*, vol. 24, pp. 721-735, 2010.
- [6] S. Yang, M. W. Sracic, and M. S. Allen, "Two algorithms for mass normalizing mode shapes from impact excited continuous-scan laser Doppler vibrometry," *Journal of Vibration and Acoustics*, vol. 134, April 2012.
- [7] S. Yang and M. S. Allen, "Output-Only Modal Analysis Using Continuous-Scan Laser Doppler Vibrometry and Application to a 20kW Wind Turbine," *Mechanical Systems and Signal Processing*, vol. Submitted April 2011, 2011.

- [8] N. M. Wereley, "Analysis and Control of Linear Periodically Time Varying Systems," PhD Thesis, *Department of Aeronautics and Astronautics*, Cambridge: Massachusetts Institute of Technology, 1991.
- [9] B. Cauberghe, "Applied Frequency-Domain System Identification in the Field of Experimental and Operational Modal Analysis," PhD Thesis, *Faculteit Tegepaste Wetenschappen, Vakgroep Werktuigkunde*, Brussels, Belgium: Vrije Universiteit Brussel, 2004.
- [10] M. S. Allen, S. Chauhan, and M. H. Hansen, "Advanced Operational Modal Analysis Methods for Linear Time Periodic System Identification," in *29th International Modal Analysis Conference (IMAC XXIX)* Jacksonville, Florida, 2011.
- [11] N. M. Wereley and S. R. Hall, "Frequency response of linear time periodic systems," Honolulu, HI, USA, 1990, pp. 3650-3655.
- [12] M. S. Allen and J. H. Ginsberg, "A Global, Single-Input-Multi-Output (SIMO) Implementation of The Algorithm of Mode Isolation and Applications to Analytical and Experimental Data," *Mechanical Systems and Signal Processing*, vol. 20, pp. 1090–1111, 2006.
- [13] J. H. Ginsberg, *Mechanical and Structural Vibrations*, First ed. New York: John Wiley and Sons, 2001.
- [14] Wang Jintian, Qu Shuying, Hou Xingmin, and Z. Jia, "Influences of Window Function on the Subsoil Damping Ratio," in *2010 International Conference on ICEEE*, pp. 1 - 4